Tree Physiology 36, 1247–1259
doi:10.1093/treephys/tpw055

Research paper

Single vessel air injection estimates of xylem resistance to cavitation are affected by vessel network characteristics and sample length

Martin D. Venturas[1,2,4], F. Daniela Rodriguez-Zaccaro[1], Marta I. Percolla[1], Casparus J. Crous[3], Anna L. Jacobsen[1] and R. Brandon Pratt[1]

[1]Department of Biology, California State University, Bakersfield, 9001 Stockdale Hwy, Bakersfield, CA 93311, USA; [2]Forest Genetics and Ecophysiology Research Group (GENFOR), School of Forest Engineering, Technical University of Madrid, 28040 Madrid, Spain; [3]Forestry and Agricultural Biotechnology Institute, University of Pretoria, Lynnwood Road & Roper Street, Hatfield, Pretoria 0002, South Africa; [4]Corresponding author (martin.venturas@gmail.com)

Received February 12, 2016; accepted May 30, 2016; published online June 29, 2016; handling Editor Frederick Meinzer

Xylem resistance to cavitation is an important trait that is related to the ecology and survival of plant species. Vessel network characteristics, such as vessel length and connectivity, could affect the spread of emboli from gas-filled vessels to functional ones, triggering their cavitation. We hypothesized that the cavitation resistance of xylem vessels is randomly distributed throughout the vessel network. We predicted that single vessel air injection (SVAI) vulnerability curves (VCs) would thus be affected by sample length. Longer stem samples were predicted to appear more resistant than shorter samples due to the sampled path including greater numbers of vessels. We evaluated the vessel network characteristics of grapevine (*Vitis vinifera* L.), English oak (*Quercus robur* L.) and black cottonwood (*Populus trichocarpa* Torr. & A. Gray), and constructed SVAI VCs for 5- and 20-cm-long segments. We also constructed VCs with a standard centrifuge method and used computer modelling to estimate the curve shift expected for pathways composed of different numbers of vessels. For all three species, the SVAI VCs for 5 cm segments rose exponentially and were more vulnerable than the 20 cm segments. The 5 cm curve shapes were exponential and were consistent with centrifuge VCs. Modelling data supported the observed SVAI VC shifts, which were related to path length and vessel network characteristics. These results suggest that exponential VCs represent the most realistic curve shape for individual vessel resistance distributions for these species. At the network level, the presence of some vessels with a higher resistance to cavitation may help avoid emboli spread during tissue dehydration.

Keywords: hydraulic architecture, plant hydraulics, water stress, water transport, xylem anatomy, xylem embolism.

Introduction

Water is transported in vascular plants from the roots to the leaves through tracheary elements under negative pressure (Dixon and Joly 1895). This passive transport mechanism is susceptible to cavitation and subsequent embolism, which occurs when a tracheary element becomes gas-filled, disrupting the soil–plant–atmosphere water continuum (Sperry and Tyree 1988, Tyree and Zimmermann 2002). As a result, the gas-filled elements become non-functional for water transport. There are several factors that can cause cavitation, such as mechanical damage, pathogens, high water demand, drought or freeze–thaw cycles (Tyree and Zimmermann 2002). Xylem resistance to cavitation is an important trait that is related to the ecology and distribution of species (Carlquist 1977, Sperry et al. 1988*b*, Maherali et al. 2004, Jacobsen et al. 2008, 2014) and drought mortality (Pratt et al. 2008, 2014, Allen et al. 2010, McDowell et al. 2011, Paddock et al. 2013).

The 'air-seeding' hypothesis explains the mechanism by which water stress causes cavitation and embolism (Sperry et al. 1988*a*, Sperry and Tyree 1988, Tyree and Zimmermann 2002).

When a sap-filled conduit is connected to a gas-filled one, gas–sap menisci form at the inter-conduit pit membrane pores. If the pressure increment between the sap (negative pressure) and gas (atmospheric pressure) is large enough to overcome the capillary force of the meniscus of the largest pit pore, a gas bubble is sucked into the sap-filled conduit through the pit pore. This gas bubble then expands until the entire conduit is gas filled. In angiosperms, the maximum pressure difference (ΔP, in MPa) that a pit membrane can withhold can be approximated by

$$\Delta P = \frac{k2\Gamma(T,P_l)\cos(\varphi)}{R_p} \quad (1)$$

where k is a dimensionless shape correction factor, $\Gamma(T, P_l)$ is the sap surface tension (N m^{-1}) at temperature T and liquid pressure P_l, φ is the contact angle of the gas–liquid interface with the pore wall and R_p is the smallest radius of the largest pore (μm) (Schenk et al. 2015). The 'rare pit' hypothesis states that the largest pit pore within any pit membrane of a conduit will determine its resistance to cavitation as per Eq. (1) (Wheeler et al. 2005, Christman et al. 2009), i.e., the bigger the largest pit pore the less resistant a conduit will be. Furthermore, the likelihood of the presence of large pit pores is partially determined by the amount of pit area of a vessel. Chemical composition of pit membranes may also be important and it has been suggested that surfactants may play a role in stability of gas bubbles (Schenk et al. 2015).

The term 'vessel network' is used to describe the pattern of connections between interconnected vessels within the xylem and it is an important xylem characteristic related to both hydraulic conductance and embolism spread. The development of techniques such as three dimensional (3D) cinematographic analysis (Zimmermann and Tomlinson 1965) and X-ray computed microtomography (Steppe et al. 2004) has improved our knowledge on how vessels are connected and distributed. Within the vessel network, connectivity refers to the number of vessels to which each vessel is connected in the network (Loepfe et al. 2007). In some angiosperm species, tracheids may also contribute to xylem connectivity (Hacke et al. 2009, Pratt et al. 2015*a*). If the connectivity is high, the chances of a functional vessel being connected to a gas-filled conduit are greater; thus, the probability of the functional vessel becoming air seeded under water stress conditions is higher. This may lead to reduced cavitation resistance. This hypothesis is similar to the rare pit hypothesis but may operate independently if the pit area of a vessel is independent of its connectivity.

Xylem resistance to water stress-induced cavitation is commonly characterized by constructing vulnerability curves (VCs) that depict the loss in hydraulic conductivity (K_h; kg MPa m s^{-1}) in relation to the xylem water potential (Ψ_x; e.g., Sperry and Saliendra 1994, Sperry et al. 2012, Hacke et al. 2015). Other methods have also used acoustic emissions (Tyree and Sperry 1989) as well as imaging to characterize conduit embolism (Holbrook et al. 2001) in relation to Ψ_x. Still other methods do not use negative pressures and instead force gas with positive pressure across pit membranes to measure cavitation resistance (Cochard et al. 1992, Sperry and Saliendra 1994) with the rationale that the pressure required to push air through an inter-conduit pit membrane is equal to the negative pressure required to pull air into the conduit when it is under tension. Early applications of this method applied positive pressure to entire organs and then measured the impact of different injection pressures on K_h. A more recent version of this method applies air to one conduit by injecting gas into it with a microcapillary. This method was first developed to measure the flow of individual xylem vessels (Zwieniecki et al. 2001) and later adapted for evaluating the relation between xylem age and the pressure threshold required to force air through the pit membranes separating individual xylem vessels (Melcher et al. 2003). Throughout this article, we will refer to the Melcher et al. (2003) modification as the single vessel air injection (SVAI) method.

Vulnerability curves acquired using the SVAI can be represented as a cumulative distribution function (CDF) of the pressure thresholds that seed air through the sample (Christman et al. 2012). Provided that the vessels that are injected are near in size to the mean hydraulic vessel diameter (VD), the pressure threshold that causes 50% of the vessel pathways to air seed will be similar to the pressure that causes 50% loss in K_h (P_{50}). However, this relationship might be affected by vessel and vessel network structure because vessels may differentially contribute to hydraulic flow if they exhibit differences in pit membrane area and conductivity, or connectivity in the context of the vessel network. It is feasible that a substantial proportion of vessels that are no longer contributing to water transport might still be water-filled when P_{50} is reached because they have become hydraulically isolated (Loepfe et al. 2007). Comparisons between the resistances to air seeding of vessel pathways and those obtained with the standard centrifuge method (Alder et al. 1997) could help elucidate how individual vessels contribute to the overall cavitation of the xylem vessel network. We examined this relationship in the present study by comparing SVAI pressure threshold distributions with standard centrifuge VCs of stems.

Published SVAI studies have used stem or root segments of different lengths, ranging from 4 to 75 cm (Melcher et al. 2003, Choat et al. 2004, Christman et al. 2012, Johnson et al. 2014, Pratt et al. 2015*b*), with sample length ultimately depending on the specific research hypothesis, the experimental design and the vessel characteristics of the analysed species. However, by altering the number of vessels in the sampled path, sample length could affect SVAI measurements. For segments shorter than the mean vessel length (VL_{mean}), there may be a large proportion of vessels open through the sample, i.e., vessels with no terminal vessel elements along the sampled pathway. This is

important to note since measurements using SVAI can only be performed on vessels that are not open through the sample, which, as segments are shortened, will be a smaller proportion of the vessels within a sample. On the other hand, using longer segments increases the probability that air is being pushed through more than one pit membrane (Figure 1). In a pathway that contains three or more vessels, air must penetrate multiple pit membranes before reaching the sample end. As injected air moves though vessel pathways, it will select the least resistant pathway by penetrating the most vulnerable pit membranes of each vessel, which are the ones damaged or with the widest pit membrane pore diameters. If vessels in a pathway differ in the air-seed pressure of their most vulnerable pit membrane, then the air-seed pressure of the pathway of several vessels will be set by the 'most resistant' of the vulnerable pit membranes along the path (Figure 1). This would result in higher resistance estimates when longer samples were measured. Thus, estimates from vessel pathways longer than two vessels will not represent the actual distribution of individual vessel air-seeding pressures. This shift has previously been reported for longer samples when one whole end of the stem was connected to tubing and injected with air (Christman et al. 2009).

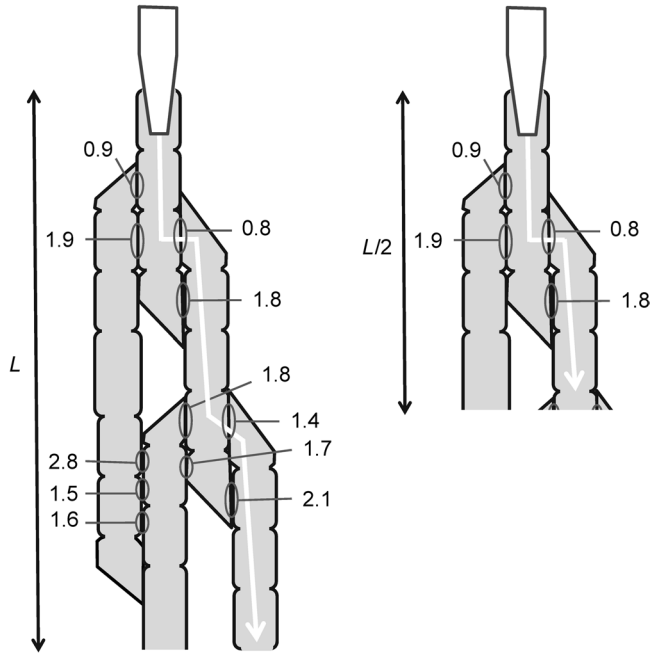

Figure 1. Diagram illustrating vessel networks within samples of differing lengths and with the most vulnerable pathway for air seeding indicated. The numbers represent the pressure in MPa that each of the inter-vessel pit membranes can withstand. These pressures were not obtained experimentally. They are hypothetical and were assigned in order to illustrate the effect of sample length on pathway seeding pressure. The microcapillary is represented at the top inserted in a vessel and the white arrow indicates the most vulnerable pathway that gas would follow for seeding through the sample. In this case, the pressure required to seed the sample of length (L) would be 1.4 MPa, whereas if the sample was trimmed to $L/2$, the pressure required would be 0.8 MPa.

The hypothesis we tested in this study was that the resistance to cavitation of individual xylem vessels differs and that the distribution of vessels with differential vulnerability are randomly distributed throughout the vessel network. Thus, we predicted that the shape of VCs constructed with the SVAI method would be affected by sample length and that this effect would be related to vessel length. Specifically, we predicted that the mean air-seed pressure would shift to being more resistant to cavitation in longer samples. We also predicted that this shift would be greater in species with shorter vessels since a greater number of inter-vessel connections would have to be seeded, and lower in samples with greater connectivity since there are more alternative low resistance pathways. The null hypothesis was that vessels do not differ in their cavitation resistance, in which case we would not find a shift in the VC shapes for samples of different lengths.

Materials and methods

Plant material

One-year-old stem samples were collected from well-watered plants growing on California State University, Bakersfield campus (35°20′N, 119°06′W, 115 m above sea level). Measurements were performed on branches of grapevine (*Vitis vinifera* L. var. 'Chardonnay', Vitaceae), English oak (*Quercus robur* L., Fagaceae) and black cottonwood (*Populus trichocarpa* Torr. & A. Gray, Salicaceae). English oak and black cottonwood trees were 3.5–6.0 m tall. Grapevine samples were collected from three plants in July 2014, English oak samples from four trees in July–August 2014 and black cottonwood samples from six trees in September–October 2014. These woody species were chosen because they have been commonly used in studies of vascular function, which facilitates comparative analyses, they all have relatively large VDs that are amenable to single vessel injection studies and they broadly differ in their vessel lengths.

Vessel length

Maximum vessel length (VL_{max}) was estimated with the air injection method (Greenidge 1952). Large branches (2–4 m) were cut in air at dawn, immediately double-bagged in plastic with moist paper towels and transported to a laboratory within 30 min from collection. In a laboratory, branches were cut under water at their distal end, in current year growth, and where the stem was 3–6 mm in diameter, which is similar to the segments we used for single vessel injection. A tube was fitted to this end of the branch that was connected to a high-pressure nitrogen tank. Stems were injected at the distal end at 100 kPa. The basal end of the branch was then submerged in a tray filled with water. Segments were cut from the basal end of the branch until the first gas bubbles were seen flowing out of a xylem vessel. The increments removed were 5 cm long if the distance to the injection point was >1.5 m and 1 cm long if the distance was <1.5 m.

The distance from the injection point to where the first air bubbles came through the stem was recorded as the VL_{max}. This method may overestimate VL_{max} in cases where air can travel through pit membranes that air seed at pressures lower than 100 kPa or that are damaged.

Vessel length distribution and VL_{mean} were evaluated using the silicone injection method (Sperry et al. 2005). Large branches were collected from the same plants and in the same manner as those collected for air injection VL_{max} measurements. In a laboratory, a 35 cm segment was cut under water from the apical end of the branch. Segments were selected so that the distal end of the segment corresponded to current year's growth and was 3–6 mm in diameter. These segments were then flushed for 1 h with an ultra-filtered (in-line filter Calyx Capsule Nylon 0.1 μm; GE Water and Process Technologies, Trevose, PA, USA) degassed 20 mM KCl solution at 100 kPa in order to refill any embolized vessels. Stem segments were injected with a two-component silicone (RhodorsilRTV-141, Rhodia USA, Cranbury, NJ, USA) containing a UV stain (Uvitex OB, Ciba Specialty Chemicals, Basel, Switzerland) dissolved in chloroform (1% by weight). One drop of the UV stain was added per gram of silicone mixture. The two-component silicone and UV stain were mixed and allowed to sit for 2 h to allow the small air bubbles incorporated during mixing to come out of the silicone. The ends of the flushed stem segments were trimmed with a fresh razor blade and the segments injected into their basal end at 50 kPa for 24 h. After the injection, the stems were cured for at least 48 h at room temperature. Prior to sectioning, stems were rehydrated to soften tissues by submerging them in water for at least 24 h. Thin cross sections (40 μm thick) were obtained with a sledge microtome (Model 860 Sledge Microtome, American Optical Corp., Buffalo, NY, USA) at distances of 0, 0.7, 1.4, 2.9, 5.8, 11.8 and 24.0 cm from the injection end. For each cross section, a total of three images at ×100 magnification were analysed for evaluating the percentage of silicone-filled vessels. These images were captured under fluorescent light with a microscope attached to a digital camera (Zeiss Stereo Discover V.12 with Axiocam HRc digital camera, Carl Zeiss Microscopy, LLC, Thornwood, NY, USA). The vessel length distribution and VL_{mean} were calculated from these measurements using the equations reported by Sperry et al. (2005). The percent of open vessels through a 5 or 20 cm segment was calculated from these same vessel distributions. The vessel density was also measured from the images of these sections by counting all the vessels present within the measured cross sections of xylem. Connectivity was evaluated from the cross section images of six samples per species. One hundred vessels were identified for each sample, and the number of vessels in direct contact with each vessel scored. Connectivity was established as the mean number of vessels to which each vessel is connected.

Vessel diameters were measured from the basal cross section of the samples (six per species) used for estimating vessel length. Images were captured at ×100 magnification with a transmission light microscope and digital camera (Axio Imager. D2 and AxioCam MRc, Carl Zeiss MicroImaging GmbH, Gottingen, Germany). For each sample, a radial section large enough to contain >100 vessels was established. The area of all vessel lumens within the radial section was measured with image analysis software (AxioVision, AxioVs40, v. 4.8.2.0, MicroImaging GmbH). Vessel diameters were calculated from these areas using the assumption that vessels were circular.

The VL_{max}, VL_{mean}, vessel density, connectivity, percentage of open vessel and VD means were compared with the Tukey–Kramer honest significant difference (HSD) test. These analyses were run in JMP 9.0.0 (SAS Institute Inc., Cary, NC, USA).

Single vessel air injection

Large branches (2–4 m) were cut in air at dawn; they were immediately double-bagged in plastic with moist paper towels and transported to a laboratory within 30 min from collection. Current year growth stem segments were exclusively used for sampling to avoid older xylem that might contain a greater number of fatigued (e.g., due to winter freeze–thaw stress) and non-functional vessels. Segments were excised under water at a distance greater than 1× the VL_{max} from the cut end. Excised segments were 20 cm for black cottonwood and oak, and 30 cm for grapevine. Sample ends were shaved with a fresh razor blade and the segments were flushed for 1 h at 100 kPa with an ultra-filtered (0.1 μm filter) 20 mM KCl degassed solution to refill any emboli. After flushing, half the oak and cottonwood samples were trimmed to 5 cm, while the other half were left at 20 cm. Because of gel formation in grapevine samples, longer samples were flushed and then central segments of 20 or 5 cm were extracted so that any gels that formed at the ends of segments during flushing were removed.

The SVAI technique described by Melcher et al. (2003) was used to determine the pressure threshold required to seed gas through a pathway of vessels in the 5 and 20 cm stem segments. These lengths were selected based on vessel length distribution. The 5 cm segments allowed for air having to seed few inter-conduit connections, whereas the 20 cm segments were about double the VL_{mean} of the two species with longer conduits. Borosilicate glass capillaries (1.5 mm outer diameter and 0.84 mm inner diameter, World Precision Instruments Inc., Sarasota, FL, USA) were pulled with a vertical capillary puller (Model P-30, Sutter Instrument Co., Novato, CA, USA). The pulled ends were cut open with a razor blade to diameters between 20 and 80 μm.

A stem segment was secured vertically under a ×40 zoom stereo microscope (Olympus Corporation, Tokyo, Japan) with a ring-stand clamp. The sample was placed so that the distal cross section could be observed through the microscope and the basal cross section was immersed in a 20 mM KCl degassed solution contained in a 150 ml glass beaker. A capillary with a

diameter slightly smaller than the lumen of the vessels to be injected was attached with a straight connector (quick-assembly brass tube fitting straight connector for 1.59 mm tube outer diameter, McMaster-Carr Co., Elmhurst, IL, USA) to 1.4 m long piece of green PEEK tubing (polyetheretherketone tubing 1.59 mm outer diameter and 0.41 mm wall thickness). The opposite end of the PEEK tube was inserted into a pressure chamber (Model 2000, PMS Instruments, Albany, OR, USA) containing a moist paper towel to humidify the chamber. The capillary was secured in a micromanipulator (Brinkmann Instruments Inc., Westbury, NY, USA) attached to a ring stand. Using the micromanipulator controls, the capillary was inserted into the lumen of a vessel. A robust seal was made by gluing the capillary to the vessel with fast drying glue (Loctite, Super Glue Gel Control, Henkel Corp., Rocky Hill, CT, USA). The chamber was pressurized at a rate of 1×10^{-3}–3×10^{-3} MPa s^{-1}. The capillaries delivered air at a rate of >1.2 ml min^{-1} at 0.05 MPa (see Figure S1 available as Supplementary Data at *Tree Physiology* Online). The sample end submerged in the beaker with degassed solution was observed until bubbles were seen coming out of a xylem vessel. The pressure at which bubbles were observed was registered as the air-seeding pressure threshold for that vessel pathway. If bubbles streamed out at pressures <0.05 MPa, it was assumed that the vessel was open through the segment, i.e., it did not contain a terminal vessel element. After each measurement, the capillary and glue were carefully removed in order to inject another vessel from the same sample. We obtained one to nine seeding pressures per stem segment. The number of open vessels was calculated for each stem segment from the number of open vessels in relation to the total number of vessels injected.

Vessels for SVAI were randomly selected throughout the xylem cross section except that we took care to avoid the row of vessels next to the pith, thereby excluding primary xylem, as well as the vessels next to the bark, which might not be fully mature (Jacobsen et al. 2015). If there was a bias, it was towards larger diameter vessels, since these enable capillaries to be inserted more easily. This could have affected our results if vessels with wider diameters are more prone to cavitation. Nevertheless, larger diameter vessels make the highest contribution to sap flow in a stem, as described by Hagen–Poiseuille law (Giordano et al. 1978), and thus these may be the most important in their impact on K_h. For grapevine, the vessels injected were in the central third of the xylem between the pith and bark since those were the ones functional and contributing to flow when the experiment was performed in July 2014 (Jacobsen et al. 2015). All SVAI measurements were performed the same day that the samples were collected.

The CDF (%) of SVAI seeding pressures, for each species and treatment (sample length), was calculated discarding open vessels and including those vessels that did not air seed at the maximum pressure that the system could sustain (~4–5 MPa). These vessels were assigned the maximum injection pressure (4.0 MPa in oak and grapevine as some capillaries broke at pressures ≥4.0 MPa, and 5.0 MPa in black cottonwood as the capillaries that broke for this species did so at pressures ≥5.0 MPa) for calculating the median air-seeding pressure (P_m), which represents the threshold at which 50% of vessel pathways air seeded. Bootstrapping was used to propagate the uncertainty and calculate the 95% confidence intervals (CIs) of P_m. To do this, 10,000 subsamples equal in size to the observed datasets (i.e., the n seeding pressures of each species) were generated by randomly resampling the observed datasets with replacement. Median air-seeding pressure was calculated for each subsample, and the percentiles 2.5 and 97.5 were used to determine the 95% CIs. In addition, a similar bootstrapping procedure was performed for determining how sample size may affect P_m estimates. Subsamples were also generated by randomly resampling with replacement. Subsamples were of size from 1 to n, and for each size, 10,000 subsamples were generated. The percentiles 2.5 and 97.5 were used to determine the 95% CIs for each sample size.

Centrifuge VCs

The branches used for constructing centrifuge VCs were collected at the same time and in the same manner as those used for SVAI measurements. The current year stems used were equal in size and vigour and came from the same plants as those used for the SVAI method. The branches were transported to a laboratory within 30 min from collection. Current year growth stem segments were excised under water and trimmed with a fresh razor blade to 14 cm for oak and black cottonwood and 20 cm for grapevine. The stem segments were located at a distance >VL_{max} from where the branches were first cut in air. The stem segments were flushed for 1 h with a 20 mM KCl degassed solution (previously described). After flushing, 3 cm were trimmed off of each end of the grapevine samples with a fresh razor blade in order to remove gels formed at the ends during flushing and for them to have a final length of 14 cm.

Hydraulic conductivity was measured gravimetrically with a conductivity apparatus (Sperry et al. 1988*a*). A low pressure head (1.5–2.0 kPa) was used to avoid displacing gas bubbles from embolized vessels. Hydraulic conductivities were corrected for background flows that can occur when no pressure head is applied (Hacke et al. 2000, Torres-Ruiz et al. 2012). Maximum K_h (K_{max}) was measured after samples were flushed. Samples were spun in an Alder et al. (1997) rotor designed to fit 14 cm stem segments. Foam pads were placed in the rotor's degassed solution reservoirs in order to avoid air-entry into stem ends while loading and unloading samples and while the centrifuge was stopped (Tobin et al. 2013). Stem segments were spun for 5 min at increasing angular velocities and their K_h remeasured following each spin. The angular velocities applied corresponded to the following xylem water potentials

(Ψ_x) in the centre of the samples: −0.25, −0.5, −1.0, −1.5, −2.0, −3.0, −4.0 and −6.0 MPa. The percent loss in K_h (PLC) for each pressure level was calculated as

$$PLC = \frac{100(K_{max} - K_h)}{K_{max}}$$

Percent loss in K_h values of each sample were fitted by least square mean errors (LSME) to a two-parameter Weibull curve:

$$PLC(\Psi_X) = 100(1 - e^{-(\Psi_X/b)^a})$$

where Ψ_x is the xylem water potential, and a and b are the shape and scale parameters to be estimated, respectively. The pressure at which 50 PLC occurs (P_{50}) was obtained for each sample from the best fit curve. The P_{50} of the three species was compared with a one-way analysis of variance (ANOVA). Xylem-specific conductivity (K_s, kg MPa m^{-1} s^{-1}) was calculated by dividing K_h by the xylem cross-sectional area of the distal end of the samples.

Modelling SVAI curve shift

The SVAI CDF curve shift in relation to the number of vessels in the injected vessel pathway was modelled. If the degree of resistance to cavitation of each vessel comes from a CDF and vessels with different degrees of resistance and that are randomly distributed through the network, then greater pressures would be required to seed air through a longer pathway. This is because more inter-conduit pit membranes have to be seeded and there is a greater chance of one of these being more resistant (Figure 1). We modelled this shift in order to see whether it was consistent with the CDF shift observed for the 5 and 20 cm segments and the vessel lengths of the three studied species. This modelled shift was based on the observed SVAI CDFs of the 5 cm segments of each species. These were fitted by LSME to a Weibull curve:

$$CDF(P) = 100(1 - e^{-(P/b)^a})$$

where P is the air-seeding pressure, and a and b are the shape and scale parameters to be estimated, respectively. We interpreted the 5 cm CDF best Weibull fit as a best approximation of the pressures required to seed one inter-vessel pit membrane in the pathway. This is a realistic interpretation based on the VL_{mean} of the species and the number of vessels that were open through these samples (Table 1). This applies especially for English oak and grapevine, although it might not be as close an approximation for black cottonwood as it had shorter vessels (Table 1). We calculated the shift for a pathway that had to seed n vessels by obtaining n random deviates from the 5 cm CDF best Weibull fit with the rweibull function of R version 3.0.2 (R Development Core Team 2013). Then, the maximum value of the n random deviates was determined as the air-seeding pressure for that pathway (P_i). We repeated this process of sampling and

Table 1. Vessels characteristics of the studied species established by microscopy and with the air injection, silicone injection and SVAI methods. *n*, sample size; VD, vessel diameter; VL_{max}, maximum vessel length; VL_{mean}, mean vessel length; *n*5, sample size of 5 cm stem segments/total number of vessels injected (open and closed); *n*20, sample size of 20 cm stem segments/total number of vessels injected (open and closed).

Species	Microscopy		Air injection		Silicone injection					SVAI		
	n	VD (μm)[1]	*n*	VL_{max} (cm)[1]	*n*	VL_{mean} (cm)[1]	Open vessels at 5 cm (%)[1]	Open vessels at 20 cm (%)[1]	Vessel density (# mm^{-2})[1]	Connectivity (#)[1]	*n*5	Open vessels at 5 cm (%)[1]	*n*20	Open vessels at 20 cm (%)[1]
Populus trichocarpa	634	28.7 ± 0.3a	5	73.9 ± 16.9a	6	1.8 ± 0.1a	0.5 ± 0.1a	0.0 ± 0.0a	272 ± 13.1c	0.92 ± 0.12b	16/62	7.7 ± 3.0a	20/62	0.0 ± 0.0a
Vitis vinifera	643	83.5 ± 1.0c	4	67.4 ± 8.6a	6	11.7 ± 1.5b	40.7 ± 5.1b	3.9 ± 1.3a	31.1 ± 1.2a	0.40 ± 0.05a	9/103	34.5 ± 7.2b	9/57	10.5 ± 3.6a
Quercus robur	662	40.9 ± 0.5b	6	83.0 ± 18.6a	6	10.9 ± 1.9b	37.1 ± 6.3b	3.6 ± 1.7a	76.4 ± 6.0b	0.41 ± 0.05a	16/229	72.5 ± 3.7c	17/114	30.7 ± 6.3b

[1]Mean ± SE; different letters within a column indicate a significant difference ($P < 0.05$) between the species' means determined by Tukey–Kramer HSD test.

establishing the P_i 1000 times. The CDF was constructed with these 1000 P_i values. We performed the previous step for each one of the species for pathways of two to six vessels ($n = 2–6$). The modelled CDF for the different pathways was plotted and compared with the 20 cm central moving mean curve. It is to be noted that the model here described is not intended to be a comprehensive one. This model represents a simplistic approach that does not take into consideration other factors such as VD, length, vessel overlap, pit membrane area or connectivity.

Results

The three studied species had different vessel network characteristics. Grapevine mean VD was twofold greater than English oak and threefold greater than black cottonwood mean VD (Table 1). Air injection VL_{max} measurements were not statistically different for the three species (Table 1). In contrast, VL_{mean} was different and cottonwood had approximately six times shorter VL_{mean} than both grapevine and English oak (Figure 2). The VL_{mean} of the latter two species was not statistically different (Table 1).

These vessel length differences were also reflected in the percentage of open vessels estimated with silicone injection for our measured sample lengths. Black cottonwood had very few open vessels through the 5 cm segments (0.5%), whereas grapevine and English oak had ~40% open through this length. There was no difference in the percentage of open vessels at 20 cm between the three species estimated with the silicone injection method (Table 1). The percentages of open vessels obtained with the SVAI method were consistent with those calculated with the silicone injection for black cottonwood and grapevine, but not for English oak. For the latter, the percentage of open vessels estimated by SVAI was 2 times greater for 5 cm segments and 8.5 times greater for 20 cm segments than the silicone injection estimates (Table 1), perhaps because SVAI vessels tended to be the wider vessels within samples. Vessel density was significantly different for all three species and was the lowest in grapevine and highest in black cottonwood (Table 1; Figure 3). Black cottonwood's connectivity was significantly higher than English oak's and grapevine's connectivity (Table 1; Figure 3).

Sample length affected the SVAI VC shape. The measured distribution of individual seeding pressures and the number of

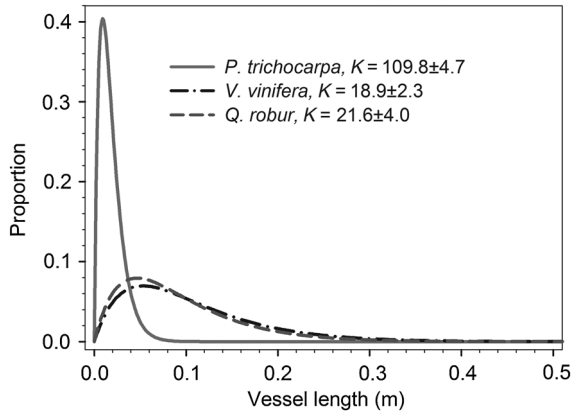

Figure 2. Vessel length distribution of the three studied species. K is the coefficient (mean ± SE, $n = 6$) of the function that represents vessel length distribution: $P_L = LK^2e^{(-KL)}$, where P_L is the proportion of vessels of length L (Wheeler et al. 2005).

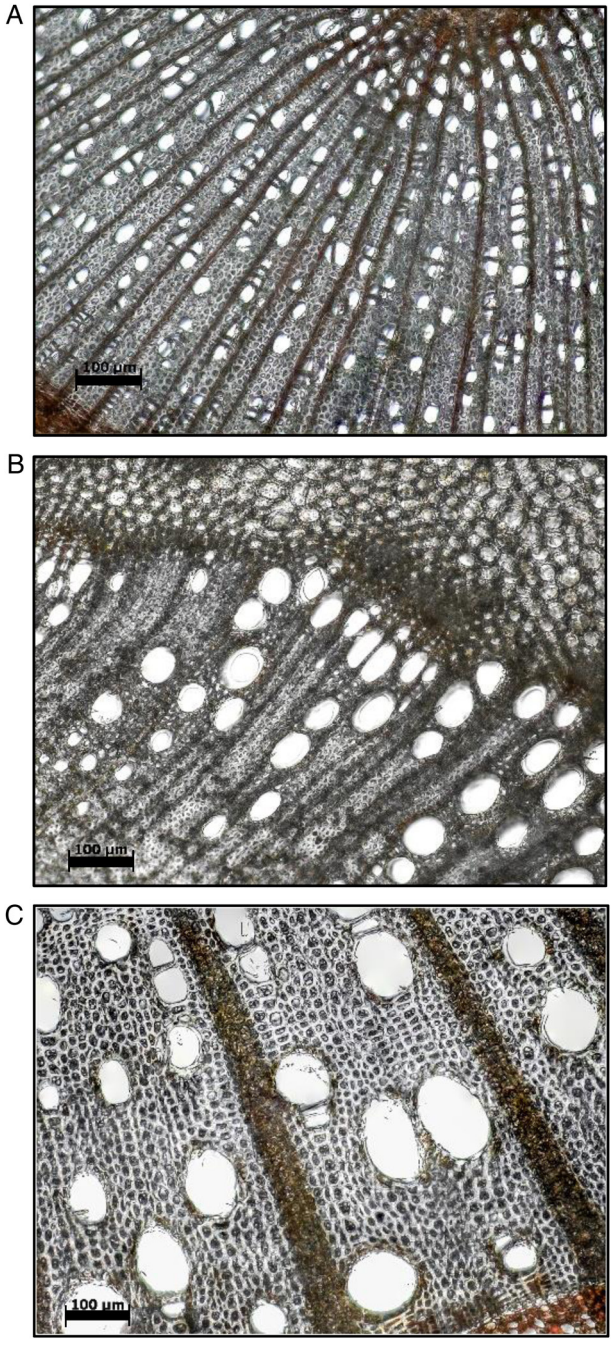

Figure 3. Representative stem xylem cross section images taken at ×100 magnification of (A) black cottonwood (*P. trichocarpa*), (B) English oak (*Q. robur*) and (C) grapevine (*V. vinifera*). Note the higher connectivity and smaller VD of black cottonwood compared with the other two species. Scale bars = 100 µm.

vessels that did not seed at maximum injection pressure are both represented in Figure 4. For all three species, the 5 cm stem segment VCs were more vulnerable than the 20 cm VCs, i.e., lower pressures were required to seed air through vessels in the 5 cm segments than the 20 cm ones (Figure 4). The P_m of 20 and 5 cm segments was significantly different in black cottonwood and grapevine. Specifically, the P_m of the 20 cm segments was 1.1 MPa higher than that of the 5 cm segments in black cottonwood, and 1.6 MPa higher in grapevine (Table 2). The P_m of English oak did not differ significantly between segment lengths (Table 2). Bootstrapping indicated that the minimum sample size for 95% CIs of P_m to stabilize was approximately from 20 to 30, depending on the curve shape (see Figure S2 available as Supplementary Data at *Tree Physiology* Online). All three species showed a proportion of pathways that could withstand greater pressures than those applied in the experiment (>4 MPa in oak and grapevine, and >5 MPa in cottonwood; Figure 4). Assigning the maximum pressure tested (4 or 5 MPa) to vessels that did not seed before that pressure does not permit calculating the mean seeding pressure but does not affect the P_m if sample size is large enough (see Figure S2 available as Supplementary Data at *Tree Physiology* Online).

The VCs obtained with the centrifuge and SVAI techniques were consistent. The VCs constructed with the centrifuge method were similar in shape to the 5 cm segments' SVAI VCs (Figure 4). Both techniques showed that there was a substantial proportion of vessels that embolized at moderate water tensions (greater than −1 MPa). The three species showed significantly different P_{50} values ($F_{2,21} = 8.0134$, $P = 0.003$; Table 2). Grapevine was the species most susceptible to xylem cavitation during dehydration and English oak the most resistant (Figure 4). However, grapevine had the highest maximum K_s, and therefore, at water potentials greater than or equal to −1 MPa, specific conductivity of grapevine was higher than that of the other two species (Figure 5). In all three species, the P_{50} values were consistent with the P_m values of the 5 cm segments (Table 2).

The modelling data supported the SVAI VC shifts observed between sample lengths. The black cottonwood 20 cm SVAI CDF was very similar to the shift expected for air having to seed five vessels in a pathway, and the English oak 20 cm SVAI curve matched the shift expected for air having to seed two vessels (Figure 6). However, grapevine's 20 cm SVAI curve only partially matched the shape of the modelled shifts; for pressures >2 MPa, the curve corresponded to the shift of air having to seed six vessels, whereas for pressures <2 MPa, it did not match any modelled curve.

Discussion

The results of this study support the hypothesis that vessels differ in their cavitation resistance. However, the second part of our hypothesis that vessels that differ in vulnerability are randomly distributed throughout the vessel network, which was tested by comparing the observed VC shifts for short and long stems with those predicted by modelling, is only partially supported. In all cases, we clearly found a shift in vulnerability to xylem cavitation between shorter and longer stem segments. For two species, English oak and black cottonwood, the observed shift was

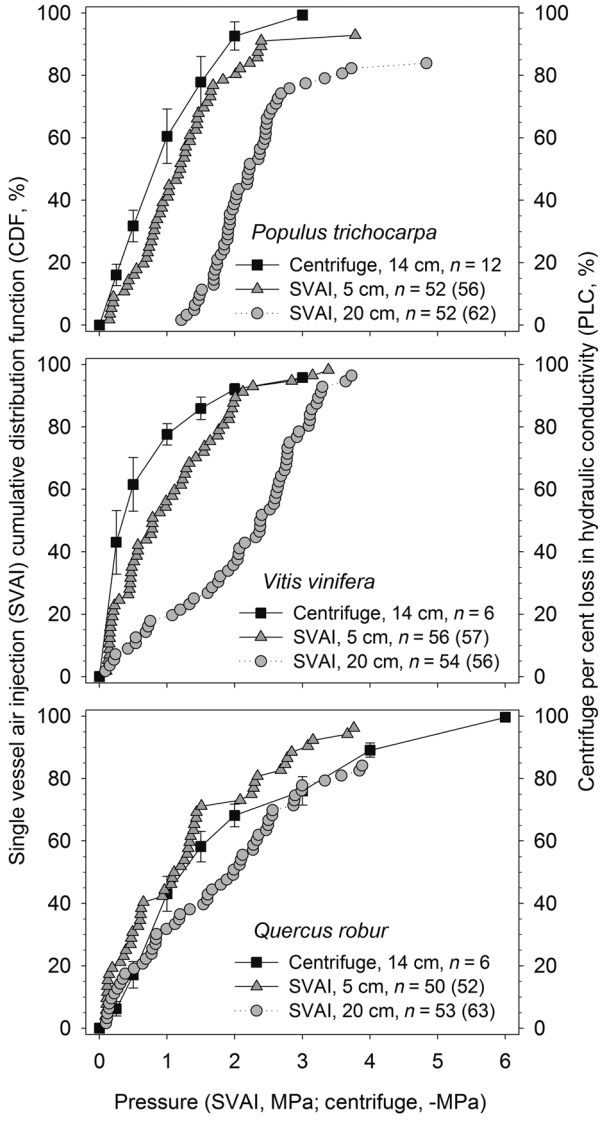

Figure 4. Xylem VCs of black cottonwood (*P. trichocarpa*), grapevine (*V. vinifera*) and English oak (*Q. robur*). For the SVAI method, the VCs are represented as the CDF for 5 cm (triangles) and 20 cm (circles) long stem segments; *n* is the number of vessel pathways with a precise measurement and the number in brackets is the total number of injected vessels that were not open through the sample over which the percentage was calculated. The remaining % from the last CDF point to 100% represents the vessels that did not seed at pressures above 5 MPa for black cottonwood and 4 MPa for grapevine and English oak. For the standard centrifuge method, the VCs are represented as the PLC (squares; means ± SE) and *n* is sample size. It is to be noted that VCs constructed with SVAI and centrifuge method cannot be directly compared as the contribution of the SVAI paths to conductivity is not directly related.

Table 2. Hydraulic properties of the studied species established with the SVAI and centrifuge methods. *L*, length of the samples; P_m, median air-seeding pressure; P_{50}, pressure that causes 50% loss in K_h.

Species	SVAI method			Centrifuge method		
	L (cm)	*N*	P_m (MPa)[1]	*L* (cm)	*n*	P_{50} (–MPa)[2]
Populus trichocarpa	5	56	1.19 (0.93, 1.43)	14	12	0.88 (0.62, 1.14)
	20	62	2.25 (1.99, 2.46)			
Vitis vinifera	5	57	0.86 (0.55, 1.23)	14	6	0.35 (–0.02, 0.72)
	20	56	2.42 (2.05, 2.67)			
Quercus robur	5	52	1.13 (0.61, 1.40)	14	6	1.36 (0.99, 1.73)
	20	63	1.97 (1.33, 2.47)			

[1]Means (95% CIs); calculated by bootstrapping. [2]One-way ANOVA least square means and 95% CIs.

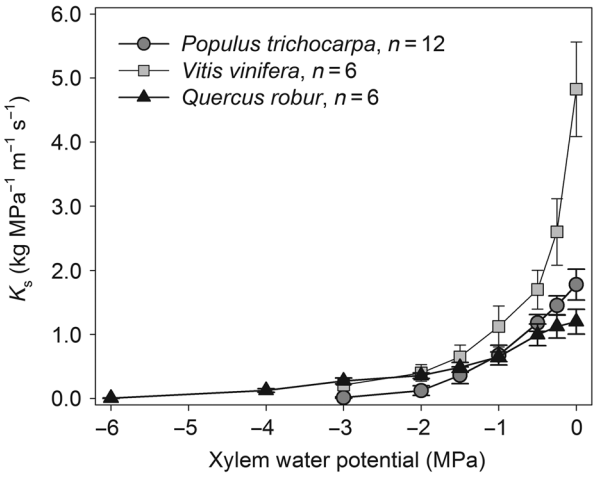

Figure 5. Xylem-specific conductivity (K_s) losses in relation to xylem water potentials for black cottonwood (*P. trichocarpa*), grapevine (*V. vinifera*) and English oak (*Q. robur*). Means ± SE are represented; *n* is sample size.

consistent with modelled shifts for pathways differing in the number of vessels having to be seeded; however, for grapevine, the shape of the SVAI curve of the long sample did not match our modelled curves well.

The lack of modelled fit for grapevine likely arises due to the characteristics of the vessel network that violate the assumptions of our model. A simple explanation is that the probability of a vulnerable vessel being connected to a more resistant one is greater than expected if they were randomly distributed. Alternatively, it may be due to air having to seed a higher number of inter-vessel pit membranes than modelled due to a non-random distribution of vessel terminations or of vessel lengths. *Vitis vinifera* has vascular tracheids that only occur at the end of growth rings; thus, vessels are not generally connected to tracheids (Carlquist 1985); however, they do have many small vessels that connect larger vessels (Brodersen et al. 2013*a*, Jacobsen et al. 2015). Grapevine has greater numbers of vessel terminations in the nodes than in the internodes (Salleo et al. 1984) and the 5 cm SVAI segments we sampled had 0.6 ± 0.2 (mean ± standard error (SE)) nodes, whereas the 20 cm segments had 2.7 ± 0.4 nodes. It is possible that the number of inter-vessel connections that have to be air-seeded in the 20 cm segments is greater than calculated from VL_{mean} measurements due to this node pattern. The presence of vessels or vascular tracheids with a higher resistance to cavitation occurring in a network of otherwise vulnerable vessels could act as security valves to help avoid emboli spreading through the entire pathway and would result in a similar pattern to the one we observed. This could provide a greater safety threshold under water stress conditions by limiting the potential for air-seeding into functional vessels, especially as the highly vulnerable pathways might not cavitate in vivo if they are not exposed to a gas-filled conduit (Christman et al. 2012). The cost of this network structure would presumably be lowered transport efficiency.

The three species analysed in this study had different vessel characteristics. Black cottonwood had shorter and narrower vessels than oak and grapevine (VD, VL_{mean}; Table 1). The grapevine VL_{mean} of our samples was nearly identical to the previously reported values for this species (Sperry et al. 2005, Jacobsen and Pratt 2012), and we are not aware of this parameter having been measured previously for English oak and black cottonwood. The latter species VL_{mean} was slightly shorter than the value reported for hybrid poplar (*P. trichocarpa* × *deltoides*) clone H11-11 seedlings, which had a VL_{mean} of 3–4 cm (Plavcová et al. 2011). Contrary to expectations, we did not find differences in VL_{max} between the three species (Table 1). Grapevine VL_{max} was consistent with previously reported data (Jacobsen and Pratt 2012), whereas Cochard et al. (2010) found English oak vessels to be 61% longer (VL_{max} = 134 cm) than our values (Table 1). This could be due to either differences in sample age, as they used up to 3-year-old shoots and VL_{max} is positively correlated with age (Jacobsen et al. 2012), differences in sample provenance or to the higher pressure they used for determining VL_{max} (0.15 vs 0.10 MPa), as some vulnerable vessels seed at pressures <0.15 MPa (Figure 4). Black cottonwood VL_{max} was previously estimated to be ~4 cm (Sparks and Black 1999), which is 18-fold shorter than the length we determined. A VL_{max} ≈ 4 cm would be more consistent with the percentage of open vessels we obtained for 5 and 20 cm segments with the silicone injection and SVAI methods (Table 1). Therefore, it is likely that our VL_{max} was overestimated, probably due to some

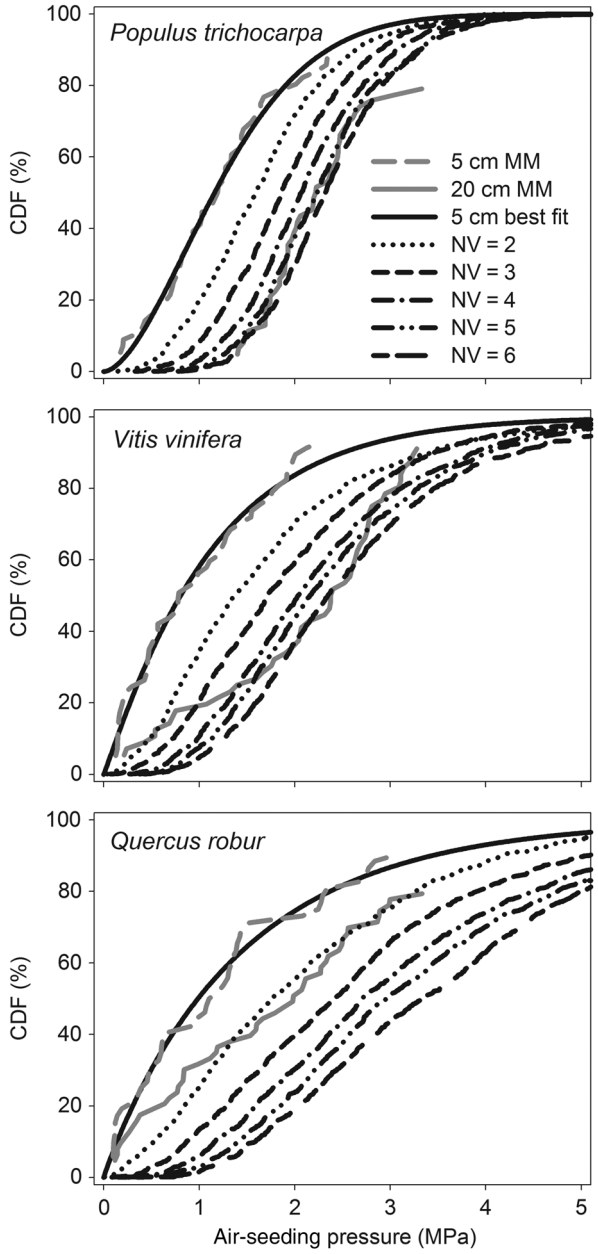

Figure 6. Single vessel air injection central moving mean curves (MM; period = 7); best Weibull fit for the CDF of the 5 cm segments and the modelled CDF shifts in relation to the number of vessels (NV) that have to be seeded in a pathway. The shifts for each NV were calculated assuming that the 5 cm CDF Weibull fit represented the CDF of the pressure threshold required for seeding one vessel. The curve for each NV was constructed with 1000 modelled data points.

pathways being seeded at pressures <0.1 MPa (Figure 4). This would also explain the differences in the percentage of open vessels calculated with silicone injection and SVAI at 5 and 20 cm for English oak and suggests that, particularly for species with a proportion of very vulnerable vessels, air injection measures for vessel length may be overestimated.

Differences among the VCs of the three studies species were consistent with their pit membrane characteristics, and these characteristics combined with vessel network characteristics are consistent with safety and efficiency patterns at the scale of whole stems. Scanning electron microscopy (SEM) and transmission electron microscopy (TEM) have been used to study pit membrane thickness and porosity (e.g., Choat et al. 2008, Jansen et al. 2009, Plavcová et al. 2011). Although SEM and TEM sample preparation affect pit membrane characteristics, and therefore measurements have to be interpreted cautiously, larger pore sizes have been correlated with greater vulnerability and thicker pit membranes with greater cavitation resistance (Jansen et al. 2009, Plavcová et al. 2011). Grapevine has thinner pit membranes, larger pit diameters and greater maximum pit pore diameter than English oak (Jansen et al. 2009), which is consistent with its greater vulnerability to cavitation (Figure 4). These pit membrane characteristics together with larger VDs may be responsible for grapevine having greater maximum K_s than oak (Figure 5) despite having lower vessel density and similar vessel length and connectivity. This is indicative of a trade-off between transport efficiency and safety (Wheeler et al. 2005, Lens et al. 2011) by which oak pit membranes have greater resistance both to sap flow and air seeding. *Populus* pit membranes are thinner and more porous than those of grapevine (Jansen et al. 2009, Plavcová et al. 2011); thus, they are expected to be more prone to air seeding. However, our VCs showed that black cottonwood was more resistant to cavitation than grapevine. Cottonwoods smaller VD and length cause lower losses in K_h when they become embolized, and the larger vessel density and connectivity provide alternative hydraulic pathways to bypass vessel blockage.

Future research could explore the effects of vessel size, density, length distribution, overlap, connectivity and pit membrane characteristics by selecting replicates of species with differences in these characteristics and injecting segments of several lengths. The development of more complex models that also include these factors and their comparison with empirical data could shed further light on the effect of vessel network characteristics on xylem resistance to cavitation. The adaptation of previously designed probabilistic models (Christman et al. 2009) or more complex models (Loepfe et al. 2007) could be an excellent point of departure to further interpret these patterns.

Vulnerability curves generated using SVAI on 5 cm samples and the standard centrifuge method were comparable within this study and to previous data for these species when samples have been processed (i.e., flushed) or scaled in a consistent manner and using plant materials of similar age and growing conditions (see Hacke et al. 2015 for a discussion of the importance of standardizing when comparing across experiments). The grapevine VC obtained in this study using a standard centrifuge method was consistent with previously reported curves that employed the same centrifuge method and K_s-based dehydration curves (Wheeler et al. 2005, Choat et al. 2010, Jacobsen

and Pratt 2012, Tobin et al. 2013, Jacobsen et al. 2015) and these data agreed with our 5 cm SVAI curves. These were also consistent with data for grapevine VCs derived from resistance models (Baert et al. 2015) and from images obtained using X-ray micro-computed tomography if the ring of vessels close to the pith is taken into consideration (Vergeynst et al. 2015), which it should be to compare flushed samples. However, our grapevine curves differ from some studies that have not similarly standardized their sampling, or used other methods (e.g., Choat et al. 2010, Brodersen et al. 2013*b*). The black cottonwood PLC values are within the range of those reported for this species using the pressure sleeve air injection method (Sparks and Black 1999) and for stems of plants subjected to drought stress (Secchi and Zwieniecki 2010). Our English oak VCs are also similar to a previously reported standard centrifuge-based curve for this species (Tobin et al. 2013) and values derived from resistance models (Baert et al. 2015). Good agreement between SVAI and VCs constructed with other techniques was also previously reported for *Quercus gambelii* Nutt. stems (Christman et al. 2012) and *Malosma laurina* (Nutt.) Nutt. ex Abrams roots (Pratt et al. 2015*b*).

The centrifuge curve represents PLC in relation to Ψ_x, whereas the SVAI curve represents the cumulative percentage of pathways that air-seed at a given pressure. The standard centrifuge peak pressure is located in the centre of the sample (Alder et al. 1997, Hacke et al. 2015). This process resembles the seeding of single vessels in the centre of the sample, which explains why the 5 cm SVAI VCs are more similar to the PLC curve than the 20 cm SVAI VCs. With the SVAI we do not know how much each of the seeded pathways contributed to flow, and this factor could also lead to potential differences between P_{50} and P_m, although we did not find a discrepancy in our study. A source of error in these comparisons might have been a sampling bias in SVAI towards vessels with greater diameters since it is easier to insert the microcapillary into them. Nevertheless, these larger vessels would be the ones that make the greatest contribution to conductivity according to Hagen–Poiseuille law (Giordano et al. 1978) and should therefore be more influential in losses in conductivity than the smaller ones.

Our results suggest that it is preferable to use short segments for the SVAI method since larger segments will overestimate the resistance of the studied organ. However, regarding methodological practicality, if segments are too short, then for some species, it could be difficult to insert the capillary into a non-open vessel. Therefore, it is important to take into consideration the VL_{mean} for selecting the most appropriate sample length for an experiment. Selection of shorter segments is likely to be particularly important for comparison with other reference methods. However, if the purpose of the experiment is to compare differences between conduits of different organs, parts of a plant, growth rings or treatments, it could be advantageous to select a longer sample length to reduce the proportion of open vessels to increase sampling efficiency. Finally, sampling schemes must also be developed that permit for a great enough sample size to be collected (>20 vessels) since the seeding pressures are highly variable (Figure 4), which results in large error values for small sample sizes (see Figure S2 available as Supplementary Data at *Tree Physiology* Online).

Both the centrifuge and SVAI methods showed a similar exponential rise for the shape of the VCs (also known as *r*-shaped curves) for the sampled species. It has been suggested that such curves are chiefly due to experimental artefacts (Cochard et al. 2010, 2013, Martin-StPaul et al. 2014). However, the agreement of these two independent methods builds on the existing studies which show that *r*-shaped VCs are indicative of the biology of some species and not due to an experimental artefact (Christman et al. 2012, Jacobsen and Pratt 2012, Sperry et al. 2012, Tobin et al. 2013, Hacke et al. 2015, Pratt et al. 2015*b*). Species with *r*-shaped curves have a large proportion of vessels that are susceptible to cavitation at moderate tensions, i.e., at high water potentials, and it is interesting to consider the selective pressures and environmental conditions that would have favoured these xylem characteristics. In these species, a large proportion of highly vulnerable vessels may only be functional during periods of high water availability, enabling them to deliver greater quantities of water to the leaves to maintain higher water potentials during transpiration and greater photosynthetic carbon gain. During periods of low water availability, the remaining resistant vessels, as well as tracheids in some angiosperm species, could sustain sufficient flow to support the physiological needs of the plant. This would be in accordance with the idea that under drought-stress periods, K_s may be more informative than PLC (Sperry et al. 2012, Hacke et al. 2015).

In summary, microcapillary single vessel injection is a powerful tool that will allow for some questions to be addressed that may not be possible to examine with other techniques. This method has been used to determine the hydraulic flow of individual vessels (Zwieniecki et al. 2001) and the hydraulic resistance of inter-vessel pit membranes (Choat et al. 2006) and of scalariform perforation plates (Christman and Sperry 2010). The SVAI modification has been used to compare the cavitation resistance of vessels of different ages within a sample (Melcher et al. 2003), and to characterize resistance to cavitation of stems (Christman et al. 2012) and roots (Johnson et al. 2014, Pratt et al. 2015*b*). Correlations between pit membrane structure and seeding pressure thresholds have also been studied with the SVAI method (Choat et al. 2004, Jansen et al. 2009). One of the drawbacks of SVAI is that it is time consuming; it can take several weeks to construct one VC, whereas with the standard centrifuge, you can build up to 12 curves a day. In addition, SVAI curves do not provide direct information on losses in conductivity, thus linking them to plant functional performance requires additional measures or simplifying assumptions. Nevertheless,

SVAI is a powerful technique, especially when its results are compared with another independent method (e.g., Melcher et al. 2003, Christman et al. 2012, Pratt et al. 2015*b*).

Supplementary data

Supplementary data for this article are available at *Tree Physiology* Online.

Acknowledgments

We are grateful to Todd McBride for lending us equipment that enabled us to perform this study. We also thank two anonymous reviewers for their comments and suggestions.

Conflict of interest

None declared.

Funding

M.D.V. acknowledges support from the Technical University of Madrid (Legado González Esparcia Grant). M.D.V., M.I.P. and R.B.P. were supported by the National Science Foundation (CAREER grant IOS-0845125). F.D.R.-Z., M.I.P. and A.L.J. were supported by the National Science Foundation (CAREER grant IOS-1252232). C.J.C. acknowledges financial support from the members of the Tree Protection Co-operative Programme (TPCP) and the DST-NRF Centre of Excellence in Tree Health Biotechnology at FABI, University of Pretoria.

References

Alder NN, Pockman WT, Sperry JS, Nuismer S (1997) Use of centrifugal force in the study of xylem cavitation. J Exp Bot 48:665–674.

Allen CD, Macalady AK, Chenchouni H et al. (2010) A global overview of drought and heat-induced tree mortality reveals emerging climate change risks for forests. For Ecol Manag 259:660–684.

Baert A, De Schepper V, Steppe K (2015) Variable hydraulic resistances and their impact on plant drought response modelling. Tree Physiol 35:439–449.

Brodersen CR, Choat B, Chatelet DS, Shackel KA, Matthews MA, McElrone AJ (2013*a*) Xylem vessel relays contribute to radial connectivity in grapevine stems (*Vitis vinifera* and *V. arizonica*; Vitaceae). Am J Bot 100:314–321.

Brodersen CR, McElrone AJ, Choat B, Lee EF, Shackel KA, Matthews MA (2013*b*) In vivo visualizations of drought-induced embolism spread in *Vitis vinifera*. Plant Physiol 161:1820–1829.

Carlquist S (1977) Ecological factors in wood evolution: a floristic approach. Am J Bot 64:887–896.

Carlquist S (1985) Observations on functional wood histology of vines and lianas: vessel dimorphism, tracheids, vasicentric tracheids, narrow vessels, and parenchyma. Aliso 11:139–157.

Choat B, Jansen S, Zwieniecki MA, Smets E, Holbrook NM (2004) Changes in pit membrane porosity due to deflection and stretching: the role of vestured pits. J Exp Bot 55:1569–1575.

Choat B, Brodie TW, Cobb AR, Zwieniecki MA, Holbrook NM (2006) Direct measurements of intervessel pit membrane hydraulic resistance in two angiosperm tree species. Am J Bot 93:993–1000.

Choat B, Cobb AR, Jansen S (2008) Structure and function of bordered pits: new discoveries and impacts on whole-plant hydraulic function. New Phytol 177:608–626.

Choat B, Drayton WM, Brodersen C, Matthews MA, Shackel KA, Wada H, McElrone AJ (2010) Measurement of vulnerability to water stress-induced cavitation in grapevine: a comparison of four techniques applied to a long-vesseled species. Plant Cell Environ 33:1502–1512.

Christman MA, Sperry JS (2010) Single-vessel flow measurements indicate scalariform perforation plates confer higher flow resistance than previously estimated. Plant Cell Environ 33:431–443.

Christman MA, Sperry JS, Alder FR (2009) Testing the 'rare pit' hypothesis for xylem cavitation resistance in three species of *Acer*. New Phytol 182:664–674.

Christman MA, Sperry JS, Smith DD (2012) Rare pits, large vessels and extreme vulnerability to cavitation in a ring-porous tree species. New Phytol 193:713–720.

Cochard H, Cruiziat P, Tyree MT (1992) Use of positive pressures to establish vulnerability curves further support for the air-seeding hypothesis and implications for pressure-volume analysis. Plant Physiol 100:205–209.

Cochard H, Herbette S, Barigah T, Badel E, Ennajeh M, Vilagrosa A (2010) Does sample length influence the shape of xylem embolism vulnerability curves? A test with the Cavitron spinning technique. Plant Cell Environ 33:1543–1552.

Cochard H, Badel E, Herbette S, Delzon S, Choat B, Jansen S (2013) Methods for measuring plant vulnerability to cavitation: a critical review. J Exp Bot 64:4779–4791.

Dixon HH, Joly J (1895) On the ascent of sap. Philos Trans R Soc B 186:563–576.

Giordano R, Salleo A, Salleo S, Wanderlingh F (1978) Flow in xylem vessels and Poiseuille's law. Can J Bot 56:333–338.

Greenidge KNH (1952) An approach to the study of vessel length in hardwood species. Am J Bot 39:570–574.

Hacke UG, Sperry JS, Pittermann J (2000) Drought experience and cavitation resistance in six shrubs from the Great Basin, Utah. Basic Appl Ecol 1:31–41.

Hacke UG, Jacobsen AL, Pratt RB (2009) Xylem function of arid-land shrubs from California, USA: an ecological and evolutionary analysis. Plant Cell Environ 32:1324–1333.

Hacke UG, Venturas MD, MacKinnon ED, Jacobsen AL, Sperry JS, Pratt RB (2015) The standard centrifuge method accurately measures vulnerability curves of long-vesselled olive stems. New Phytol 205:116–127.

Holbrook NM, Ahrens ET, Burns MJ, Zwieniecki MA (2001) In vivo observation of cavitation and embolism repair using magnetic resonance imaging. Plant Physiol 126:27–31.

Jacobsen AL, Pratt RB (2012) No evidence for an open vessel effect in centrifuge-based vulnerability curves of a long-vesselled liana (*Vitis vinifera*). New Phytol 194:982–990.

Jacobsen AL, Pratt RB, Davis SD, Ewers FW (2008) Comparative community physiology: nonconvergence in water relations among three semi-arid shrub communities. New Phytol 180:100–113.

Jacobsen AL, Pratt RB, Davis SD, Tobin MF (2014) Geographic and seasonal variation in chaparral vulnerability to cavitation. Madroño 61:317–327.

Jacobsen AL, Pratt RB, Tobin MF, Hacke UG, Ewers FW (2012) A global analysis of xylem vessel length in woody plants. Am J Bot 99:1583–1591.

Jacobsen AL, Rodriguez-Zaccaro FD, Lee TF, Valdovinos J, Toschi HS, Martinez JA, Pratt RB (2015) Grapevine xylem development, architecture and function. In: Hacke UG (ed.) Functional and ecological xylem anatomy. Springer, New York, pp 133–162.

Jansen S, Choat B, Pletsers A (2009) Morphological variation of intervessel pit membranes and implications to xylem function in angiosperms. Am J Bot 96:409–419.

Johnson DM, Brodersen CR, Reed M, Domec J-C, Jackson RB (2014) Contrasting hydraulic architecture and function in deep and shallow roots of tree species from a semi-arid habitat. Ann Bot Lond 113:617–627.

Lens F, Sperry JS, Christman MA, Choat B, Rabaey D, Jansen S (2011) Testing hypotheses that link wood anatomy to cavitation resistance and hydraulic conductivity in the genus *Acer*. New Phytol 190:709–723.

Loepfe L, Martinez-Vilalta J, Piñol J, Mencuccini M (2007) The relevance of xylem network structure for plant hydraulic efficiency and safety. J Theor Biol 247:788–803.

Maherali H, Pockman WT, Jackson RB (2004) Adaptive variation in the vulnerability of woody plants to xylem cavitation. Ecology 85:2184–2199.

Martin-StPaul NK, Longepierre D, Huc R, Delzon S, Burlett R, Joffre R, Rambal S, Cochard H (2014) How reliable are methods to assess xylem vulnerability to cavitation? The issue of 'open vessel' artifact in oaks. Tree Physiol 34:894–905.

McDowell NG, Beerling DJ, Breshears DD, Fisher RA, Raffa KF, Stitt M (2011) The interdependence of mechanisms underlying climate-driven vegetation mortality. Trends Ecol Evol 26:523–532.

Melcher PJ, Zwieniecki MA, Holbrook NM (2003) Vulnerability of xylem vessels to cavitation in sugar maple. Scaling from individual vessels to whole branches. Plant Physiol 131:1775–1780.

Paddock WAS III, Davis SD, Pratt RB, Jacobsen AL, Tobin MF, López-Portillo J, Ewers FW (2013) Factors determining mortality of adult chaparral shrubs in an extreme drought year in California. Aliso 31:49–57.

Plavcová L, Hacke UG, Sperry JS (2011) Linking irradiance-induced changes in pit membrane ultrastructure with xylem vulnerability to cavitation. Plant Cell Environ 34:501–513.

Pratt RB, Jacobsen AL, Mohla R, Ewers FW, Davis SD (2008) Linkage between water stress tolerance and life history type in seedlings of nine chaparral species (Rhamnaceae). J Ecol 96:1252–1265.

Pratt RB, Jacobsen AL, Ramirez AR, Helms AM, Traugh CA, Tobin MF, Heffner MS, Davis SD (2014) Mortality of resprouting chaparral shrubs after a fire and during a record drought: physiological mechanisms and demographic consequences. Glob Change Biol 20:893–907.

Pratt RB, Percolla MI, Jacobsen AL (2015*a*) Integrative xylem analysis of chaparral shrubs. In: Hacke UG (ed.) Functional and ecological xylem anatomy. Springer, New York, pp 189–207.

Pratt RB, MacKinnon ED, Venturas MD, Crous CJ, Jacobsen AL (2015*b*) Root resistance to cavitation is accurately measured using a centrifuge technique. Tree Physiol 35:185–196.

R Development Core Team (2013) R: a language and environment for statistical computing. R Foundation for Statistical Computing, Vienna, Austria. http://www.R-project.org (2 June 2014, date last accessed).

Salleo S, Lo Gullo MA, Siracusano L (1984) Distribution of vessel ends in stems of some diffuse- and ring-porous trees: the nodal regions as 'safety zones' of the water conducting system. Ann Bot Lond 54:543–552.

Schenk HJ, Steppe K, Jansen S (2015) Nanobubbles: a new paradigm for air-seeding in xylem. Trends Plant Sci 20:199–205.

Secchi F, Zwieniecki MA (2010) Patterns of PIP gene expression in *Populus trichocarpa* during recovery from xylem embolism suggest a major role for the PIP1 aquaporin subfamily as moderators of refilling process. Plant Cell Environ 33:1285–1297.

Sparks JP, Black RA (1999) Regulation of water loss in populations of *Populus trichocarpa*: the role of stomatal control in preventing xylem cavitation. Tree Physiol 19:453–459.

Sperry JS, Saliendra NZ (1994) Intra- and inter-plant variation in xylem cavitation in *Betula occidentalis*. Plant Cell Environ 17:1233–1241.

Sperry JS, Tyree MT (1988) Mechanism of water stress-induced xylem embolism. Plant Physiol 88:581–587.

Sperry JS, Donnelly JR, Tyree MT (1988*a*) A method for measuring hydraulic conductivity and embolism in xylem. Plant Cell Environ 11:35–40.

Sperry JS, Tyree MT, Donnelly JR (1988*b*) Vulnerability of xylem to embolism in a mangrove vs an inland species of Rhizophoraceae. Physiol Plant 74:276–283.

Sperry JS, Hacke UG, Wheeler JK (2005) Comparative analysis of end wall resistivity in xylem conduits. Plant Cell Environ 28:456–465.

Sperry JS, Christman MA, Torres-Ruiz JM, Taneda H, Smith DD (2012) Vulnerability curves by centrifugation: is there an open vessel artefact, and are 'r' shaped curves necessarily invalid? Plant Cell Environ 35:601–610.

Steppe K, Cnudde V, Girard C, Lemeur R, Cnudde J-P, Jacobs P (2004) Use of X-ray computed microtomography for non-invasive determination of wood anatomical characteristics. J Struct Biol 148:11–21.

Tobin MF, Pratt RB, Jacobsen AL, De Guzman ME (2013) Xylem vulnerability to cavitation can be accurately characterised in species with long vessels using a centrifuge method. Plant Biol 15:496–504.

Torres-Ruiz JM, Sperry JS, Fernández JE (2012) Improving xylem hydraulic conductivity measurements by correcting the error caused by passive water uptake. Physiol Plant 146:129–135.

Tyree MT, Sperry JS (1989) Vulnerability of xylem to cavitation and embolism. Annu Rev Plant Biol 40:19–36.

Tyree MT, Zimmermann MH (2002) Xylem structure and the ascent of sap, 2nd edn. Springer, Berlin, Germany, pp 49–141, 229–257.

Vergeynst LL, Dierick M, Bogaerts JAN, Cnudde V, Steppe K (2015) Cavitation: a blessing in disguise? New method to establish vulnerability curves and assess hydraulic capacitance of woody tissues. Tree Physiol 35:400–409.

Wheeler JK, Sperry JS, Hacke UG, Hoang N (2005) Inter-vessel pitting and cavitation in woody Rosaceae and other vesselled plants: a basis for a safety versus efficiency trade-off in xylem transport. Plant Cell Environ 28:800–812.

Zimmermann MH, Tomlinson PB (1965) Anatomy of the palm *Rhapis excelsa*. I. Mature vegetative axis. J Arnold Arbor 46:160–180.

Zwieniecki MA, Melcher PJ, Holbrook NM (2001) Hydraulic properties of individual xylem vessels of *Fraxinus americana*. J Exp Bot 52:257–264.